Seasonal Transport Variation in the Western Subtropical North Atlantic: Experiments with an Eddy-resolving Model

CLAUS W. BÖNING, RALF DÖSCHER AND REINHARD G. BUDICH

Institut für Meereskunde, an der Universität Kiel, Germany

(Manuscript received 27 July 1990, in final form 23 November 1990)

ABSTRACT

A high-resolution model of the wind-driven and thermohaline circulation in the North and equatorial Atlantic Ocean is used to study the structure and variability of the boundary current system at 26°N, including the Florida Current, the Antilles Current, and the Deep Western Boundary Current (DWBC). The model was developed by Bryan and Holland as a Community Modeling Effort of the World Ocean Circulation Experiment. Subsequent experiments have been performed at IfM Kiel, with different friction coefficients, and different climatologies of monthly mean wind stress: Hellerman–Rosenstein (HR) and Isemer–Hasse (IH). The southward volume transports in the upper 1000 m of the interior Atlantic, at 26°N, are 25.0 Sv (Sv $\equiv 10^6$ m^3 s^{-1}) for HR, and 34.9 Sv for IH forcing, in good agreement with the transport from the integrated Sverdrup balance at this latitude (23.9 Sv for HR, 35.6 Sv for IH). The return flow of this wind-driven transport, plus the southward transport of the DWBC (6–8 Sv), is partitioned between the Florida Current and Antilles Current. With HR forcing, the transport through the Straits of Florida is 23.2 Sv; this increases to 29.1 Sv when the wind stresses of IH are used. The annual variation of the simulated Florida Current is very similar to previous, coarse-resolution models when using the same wind-stress climatology (HR); the annual range (3.4 Sv) obtained with HR forcing is strongly enhanced (6.3 Sv) with IH forcing. The meridional heat transport at 26°N, zonally integrated across the basin, is in phase with the Florida Current; its annual range increases from 0.44 PW (HR) to 0.80 PW (IH). The annual signal east of the Bahamas is masked by strong transport fluctuations on a time scale of O(100 days), caused by an instability of the Antilles Current. By averaging over several model years, an annual cycle is extracted, which is in phase with the wind stress curl over the western part of the basin.

1. Introduction

The boundary currents in the western subtropical North Atlantic, including the Florida Current, the Antilles Current, and the Deep Western Boundary Current (DWBC), have been a focal point of various field programs and model studies in recent years. The current system to the west and east of the Bahamas represents a signature of both the wind-driven and the thermohaline component of large-scale circulation, contributing a large signal in the poleward oceanic heat transport. A question of particular interest is how the variability of the current system is related to regional and basinwide processes. This question is investigated here by means of a high-resolution model of the wind-driven and thermohaline circulation in the North Atlantic. The model has been developed as a first Community Modeling Effort of the World Ocean Circulation Experiment (Bryan and Holland 1989). Here we shall examine the transport variation in a series of model experiments, which were particularly aimed at the sensitivity of the circulation to the wind forcing.

A large fraction of the northward flow in the subtropical North Atlantic is carried through the Straits of Florida. Various observational programs have been devoted to measure the flow through this natural "bottleneck" of the circulation and its variability on different time scales (Schmitz and Richardson 1968; Niiler and Richardson 1973; Larsen and Sanford 1985; Leaman et al. 1987; Schott et al. 1988). There is a well-established picture of an annual mean transport of 29–32 Sv (1 Sv $\equiv 10^6$ m^3 s^{-1}) with an annual range of variation of 6–7 Sv, providing a stringent test for any model of the North Atlantic circulation. A prominent feature of the observations is the rapid drop from a maximum transport in July–August to a minimum in October–November.

At present the sources of the mean transport as well as the cause of the seasonal variation are under debate. The annual mean transport of the Florida Current was found to be in reasonable agreement with the southward transport from the integrated Sverdrup balance across the ocean interior (Leetma et al. 1977), establishing a view of the Florida Current as the return flow of the wind-driven subtropical gyre. This conclusion was challenged by Wunsch and Roemmich (1985), noting an inconsistency with existing estimates of the meridional transport of heat. The estimates of Sverdrup transport also depend on the particular wind-stress field

Corresponding author address: Dr. Claus Böning, Institut für Meereskunde, Düsternbrooker Weg 20, D-2300 Kiel 1, Federal Republic of Germany.

under consideration. Recent comparisons of various wind-stress climatologies, based on different parameterizations and data sources, show differences of up to a factor of 2 in the region of the northeast trades (Harrison 1989; Chelton et al. 1990; Böning et al. 1990).

Another contribution to the Florida Current may arise from the upper-layer return flow of the thermohaline cell in the Atlantic. The southward transport of North Atlantic Deep Water (NADW) is in the range of 10–15 Sv as estimated from hydrographic data (Hall and Bryden 1981; Wunsch 1984) or global water-mass analysis (Gordon 1986). Recent current measurements east of Abaco, Bahamas, at 26.5°N show a strong DWBC with a mean southward transport of 33 Sv (Lee et al. 1990) and 35 Sv (Leaman and Harris 1990), respectively, indicating that the DWBC may be enhanced locally by a deep cyclonic recirculation. The deep southward flow of NADW has to be balanced by a northward transport of South Atlantic (SA) water masses. Hydrographic data suggest a spreading of SA waters through the Caribbean to the Florida Straits (Roemmich and Wunsch 1985; Schmitz and Richardson 1990), but give no indication of such water masses to the east of the Bahamas (Olson et al. 1984).

The particular amplitude and phase of the seasonal transport variation in the Florida Straits has been of considerable interest for theoretical studies and modeling exercises. It had been noted by Gill and Niiler (1973) that, in midlatitudes, the seasonal and mean responses to the large-scale wind stress cannot be the same since the time scale for establishing the mean fields are much longer than a year. Anderson and Killworth (1977) and Anderson et al. (1979) studied the mechanisms by which a mean wind-driven circulation in a stratified ocean is established: initially the response is barotropic and does not satisfy the (nontopographic) Sverdrup balance. The effect of topography is compensated, and the Sverdrup balance is established only after the time taken for the baroclinic Rossby waves to cross the basin.

The various processes affecting the annual variation of boundary current transport have been illustrated, within the context of an idealized model, by Anderson and Corry (1985a). Unless forcing adjacent to the western boundary is considered, baroclinic Rossby waves had only little effect on transport variations in midlatitudes. The seasonal response to the large-scale forcing is essentially barotropic, namely, that for a homogeneous ocean, and thus strongly influenced by topography; the phase lag is roughly zero. The barotropic signal is blocked by the topography of the Antilles–Bahamas island arc. Two mechanisms other than the large-scale wind stress curl (which has its maximum in January) were identified to be of possible relevance for the seasonal variation of the Florida Current: wind stress over varying topography, and the passage of a coastally trapped baroclinic wave, excited to the north of the Straits by the alongshore wind stress.

The relative importance of these processes was examined by Anderson and Corry (1985b; hereafter AC) with a linear, two-layer model of the North Atlantic Ocean. The time-varying part of the circulation was forced with the monthly mean wind-stress anomalies of Hellerman and Rosenstein (1983; hereafter HR). The model successfully reproduced the phase of the observed transport variation, but underestimated the amplitude by a factor of 2. Both forcing over the Caribbean and in the western Atlantic, north of the Florida Straits, contributed to the seasonal variation. A similar seasonal cycle was obtained by Greatbatch and Goulding (1989, hereafter GG) with a linear one-layer model, and by Smith et al. (1990; hereafter SBB) with a model formulated in isopycnic coordinates.

A common feature of seasonally forced models, including AC, GG, SBB, and Sarmiento (1986), is a strong annual variation of ±(10–15 Sv) east of the Bahamas. The maximum northward transport occurs in January, the minimum in October, roughly in phase with the wind-stress curl over the subtropical North Atlantic. This apparently robust model result stands in sharp contrast to observational evidence. The current measurements of Lee et al. (1990), taken at 26.5°N over a 14-month period, gave no indication of an annual signal; instead, they showed a surprisingly large (90 Sv) variation of the volume transport on a time scale of approximately 100 days.

In this paper we shall examine the transport variation of the boundary current system in a high-resolution, primitive equation model of the North Atlantic wind-driven and thermohaline circulation. The model was initially developed at NCAR as a first Community Modeling Effort of the World Ocean Circulation Experiment (Bryan and Holland 1989). Subsequent experiments were run at IfM Kiel aiming mainly at the model sensitivity to different wind-stress climatologies (Böning et al. 1990). The main focus here will be on the flow through sections at 26°–27°N, allowing an evaluation of the model against the observations west and east of the Bahamas. It had been noted already (Böning et al. 1990) that the model forced by HR shows a seasonal variation of the Florida Straits transport very similar to the results of the more idealized models mentioned above. The annual amplitude is increased by nearly a factor of 2 when the wind-stress climatology of Isemer and Hasse (1987, hereafter IH) is used, bringing the model to much better agreement with the observational evidence.

The paper is organized as follows: in section 2 we briefly review the model configuration and describe the experiments. In section 3 the spatial structure and temporal variability of the model velocity field in the western subtropical NA are described. The transport through the Straits of Florida and its sensitivity to the wind forcing are examined in section 4. Section 5 addresses the question of a seasonal cycle to the east of the Bahamas. In section 6 we examine the mean trans-

port balance of the wind-driven and thermohaline circulation for a transatlantic section at 26°N. The seasonal cycle of the meridional heat transport is analyzed in section 7 and compared with the observational evidence.

2. The model experiments

The high-resolution model of the wind-driven and thermohaline circulation has been developed by Bryan and Holland (1989) based on the primitive equation model described by Bryan (1969) and Cox (1984). The initial experiment performed at NCAR was a 25-year simulation of the North Atlantic circulation starting from initial conditions given by the climatology of Levitus (1982). A description is given by Bryan and Holland (1989). Based on this first experiment is a sequence of model runs at IfM Kiel focusing on the model sensitivity to changes in wind forcing and frictional parameters (Fig. 1).

The model domain extends from 15°S to 65°N, the latitudinal grid spacing is 1/3°, the longitudinal grid spacing is 0.4°. There are 30 levels in the vertical; the vertical grid spacing increases smoothly from 35 m at the surface to 100 m near 500 m and 250 m below 1000 m. The thermohaline circulation is driven by a relaxation of surface salinity to the monthly mean values of Levitus and a heat flux given by the linear formulation of Han (1984). An important factor determining the strength of the thermohaline cell is the formulation of the boundary conditions at the northern and southern boundaries. The model relies on a technique, which had been used with reasonable success in previous calculations with this type of model (Sarmiento 1986). Near the boundaries, closed to normal flow, buffer zones are incorporated in which temperature and salinity are restored to the seasonally varying Levitus (1982) climatology. In this way, the southern buffer zone aims at an artificial transformation of southward-flowing NADW into warm, northward-flowing upper-layer water. Obviously the strength of the meridional overturning cell thus depends on the effectiveness by which this restoring process is accomplished.

The initial experiment at NCAR (NCAR 1) was forced with the monthly mean wind stresses of HR. Constant eddy coefficients for vertical viscosity (30 cm^2 s^{-1}) and diffusivity (0.3 cm^2 s^{-1}), and constant coefficients (-2.5×10^{19} cm^4 s^{-1}) for the biharmonic lateral friction and diffusivity were used.

The experiments conducted at IfM Kiel are summarized in Fig. 1. Our first experiment (KIEL 1) was initialized with the model fields of year 16.5 of NCAR 1 and integrated, with a reduced vertical viscosity (10 cm^2 s^{-1}), through model year 24. A major effect of this change could be seen in the structure of the equatorial current system (Schott and Böning 1990). The last 5 years of this experiment were repeated, then

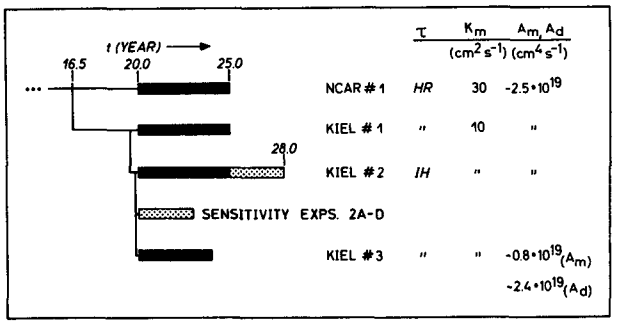

FIG. 1. Schematic of the experiments with the high-resolution Atlantic model. The experiments conducted at IfM Kiel were initialized with model year 16.5 of the original NCAR experiment (Bryan and Holland 1989). KIEL 1 was based on the same model configuration as NCAR 1, except for the coefficient of vertical viscosity (K_m). KIEL 2 was forced by the wind stresses of Isemer and Hasse (1987; IH), instead of Hellerman and Rosenstein (1983; HR). In KIEL 3 the coefficients of the biharmonic horizontal diffusion (A_m of momentum, A_d of temperature and salinity) were lowered to the values used by Cox (1985) in his eddy-resolving study of a box ocean. In the sensitivity experiments 2A to 2D the seasonal variation of wind stress was eliminated in certain model regions.

(KIEL 2) forced by the wind-stress climatology of IH. Later we added three more years to monitor the equilibration process, e.g., of the Florida Straits transport, over a longer period of time. In a series of shorter experiments (2A–D) we examined the influence of the seasonal wind forcing and of different forcing regions on the variability of the boundary currents. Finally KIEL 2 was repeated with reduced lateral friction (KIEL 3). We used the same coefficients here as Cox (1985) in his pioneering eddy-resolving study of a primitive equation ocean with idealized (box) geometry.

A detailed comparison of the wind-stress climatologies of HR and IH is given by Böning et al. (1990). Both climatologies are based on surface marine datasets and application of the bulk aerodynamic formula to the individual observations. Differences between the stress fields are mainly caused by two basic assumptions: the choice of the drag coefficients and of the Beaufort equivalent scale.

The drag coefficients adopted by HR are essentially those introduced by Bunker (1976). The drag coefficients used by IH are based on a collection of more recent experimental results (e.g., Smith 1980; Large and Pond 1981), leading to a 21% reduction compared to the values of HR. However, the reduction of the wind stress for a given wind speed is effectively counteracted in IH by a simultaneous revision of the Beaufort equivalent scale used to decode ship estimates of Beaufort force to wind speed. Instead of the official WMO scale, code 1100, which has long been suspected of systematic errors (WMO 1970), IH used a scientific Beaufort scale, which had been derived by comparing a large number of individual Beaufort estimates from ships with simultaneous wind speed measurements

taken at nearby ocean weather ships (Kaufeld 1981). A major effect of the revised scale is a substantial increase of wind speeds for small Beaufort numbers, leading to larger values of wind stress, mainly in the trades.

3. Circulation patterns in the subtropical western North Atlantic

a. Structure of the mean flow

The model configuration of islands and passages between the western North Atlantic and the Caribbean Sea is illustrated in Fig. 2, showing vectors of the 5-year mean velocity field at model level 6 (232 m) and level 17 (2125 m). There is no major difference in the circulation pattern between experiments KIEL 1 and 2. The prominent feature of the deeper layer is the DWBC, which appears as a continuous current along the Antilles island arc. Core velocities are about 10 cm s^{-1}. In some regions, e.g., to the east of the Bahamas at 27°N, the DWBC is associated with small cyclonic recirculation gyres, which locally enhance the southward boundary current.

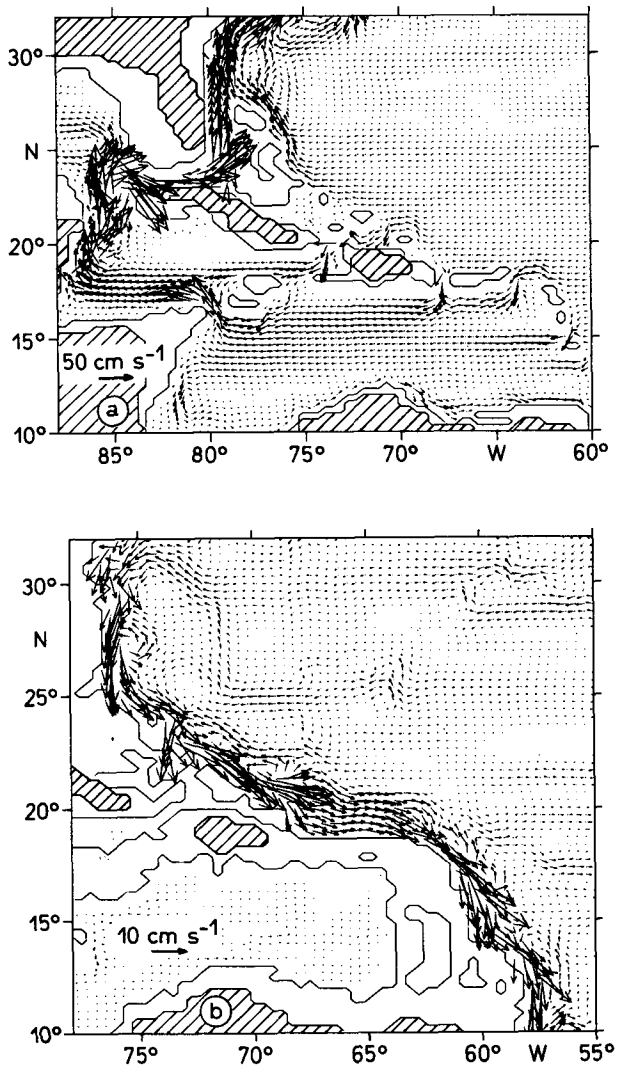

FIG. 2. Mean velocity vectors in the subtropical western Atlantic and Caribbean Sea: Experiment KIEL 2. (a) Model level 6 (232 m), (b) level 17 (2125 m).

In the upper layer, the bulk of the northward flow is carried through the Straits of Florida. The contribution to the Florida Current by flow between the Bahamas and Cuba is negligible (transports are less than 0.1 Sv); thus, the volume transport through the Straits of Florida is related to the inflow into the Caribbean Sea through the passages between Cuba and South America. To the east of the Bahamas, the model predicts an Antilles Current with a subsurface (~300-m depth) core and maximum speed of 30 cm s^{-1}. There is only little evidence of an anticyclonic recirculation near the boundary as indicated by observations. The Antilles Current in the model appears as a part of the subtropical gyre.

The vertical structure of the boundary currents is shown with zonal cross sections of the mean meridional velocity $\bar{v}$ and salnity $\bar{S}$ (Fig. 3). The Florida Current is resolved by three velocity points in cross direction; current speeds at the surface exceed 100 cm s^{-1}. Similar to observations (Leaman et al. 1987), the model current exhibits an asymmetric velocity profile with highest velocities at the western side of the straits. The salinity section and T–S profiles (Fig. 4) also compare quite reasonably with the observed structure (Roemmich and Wunsch 1985). We can identify basically three water masses: a thin layer of relatively fresh warm water, overlying the colder salinity-maximum water (SMW) of subtropical North Atlantic origin, with a core (>36.4 psu) on the eastern side of the straits; near the bottom salinity decreases below 35.0 psu indicating a contribution of Antarctic Intermediate Water (AAIW). The T–S profiles of the model show less pronounced extrema than the observations.

The AAIW enters the Caribbean Sea mainly through the southernmost model passages (south of Guadaloupe). Figure 5 gives a meridional cross section at 63.6°W. The core of AAIW is located in the southern portion of the Caribbean, at 700–800-m depth. In the same section, the SMW with core salinities of >36.8 psu is found at positions farther north, in 150–200-m depth. On top of this the model shows a thin surface layer of low salinity water (<35.1 psu) (which is not surprising since surface salinity is relaxed to the values given by Levitus). The observed salinity structure has been interpreted by Schmitz and Richardson (1990) as a signature of water of South Atlantic origin, finding its way through the southern passages of the Lesser Antilles. They estimate that ~7 Sv of the surface water, plus ~6 Sv of the deeper (AAIW) water, which are transported through the Florida Straits, are of South Atlantic origin. The present model quantitatively differs from this observational picture: the analysis of Schott and Böning (1990) indicates only a weak connection

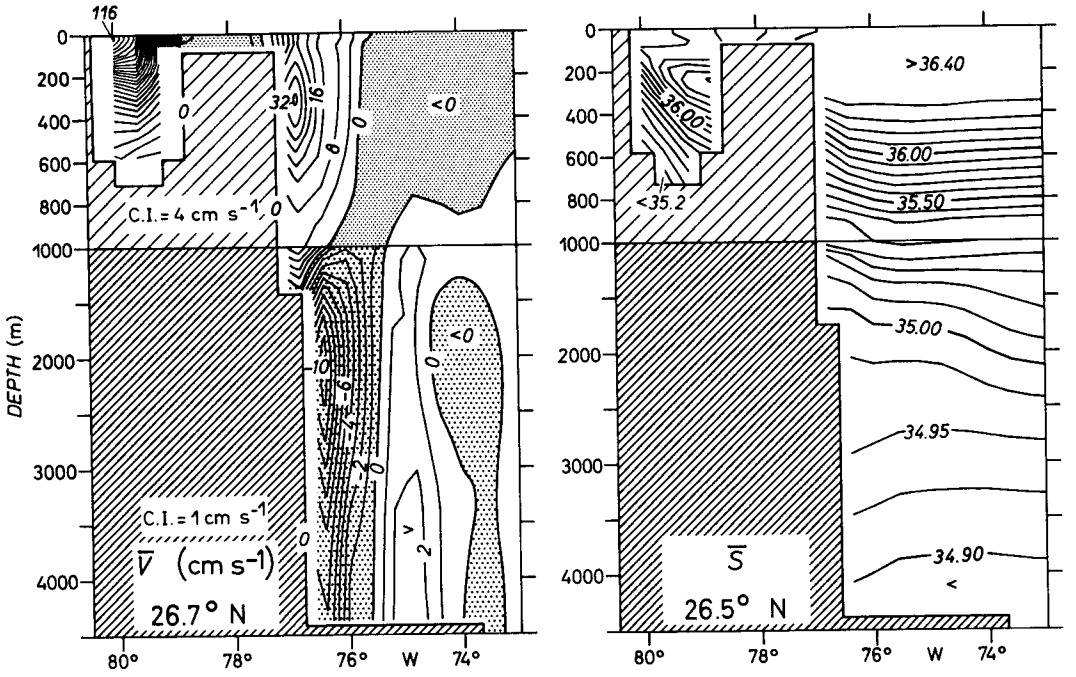

FIG. 3. Mean meridional velocity component $\bar{v}$ and salinity $\bar{S}$ in zonal sections at 26.7° and 26.5°N: experiment KIEL 2. Areas of southward velocity are stippled. Different contour intervals are used above and below 1000 m.

between the equatorial Atlantic and the Caribbean Sea. Through the passages south of Martinique (14°N) only 5 Sv enter the Caribbean in the upper 206 m, and 2 Sv in the layers below 519 m.

b. *Variability of the boundary currents*

Figure 6 shows longitude–time plots of the meridional velocity component at 27°N. In both experiments using the comparatively high horizontal friction (KIEL 1 and 2), the Florida Current exhibits a clear seasonal signal (Fig. 6a). Highest velocities (>130 cm s^{-1} in KIEL 2) are obtained in July, and a minimum (<100 cm s^{-1}) in October. With reduced horizontal friction (KIEL 3; Fig. 6b) the current becomes unstable; fluctuations of shorter period begin to develop and superimpose the seasonal signal. Maximum velocities in this experiment barely exceed 100 cm s^{-1}.

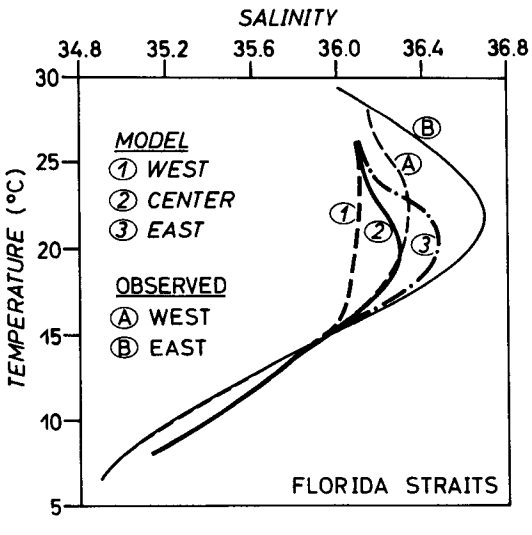

FIG. 4. *T–S* profiles in the Florida Straits at 26.5°N, for the western (1), the middle (2), and the eastern (3) model grid point. The thin lines are observed profiles from Schmitz and Richardson (1990).

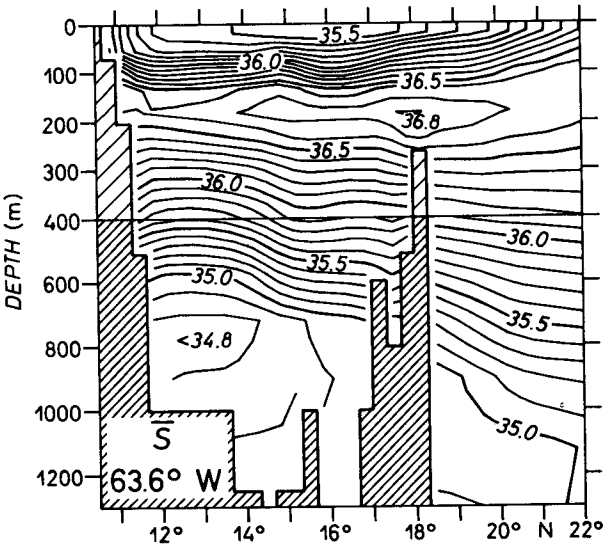

FIG. 5. Mean salinity in a meridional section through the Caribbean Sea at 63.6°W.

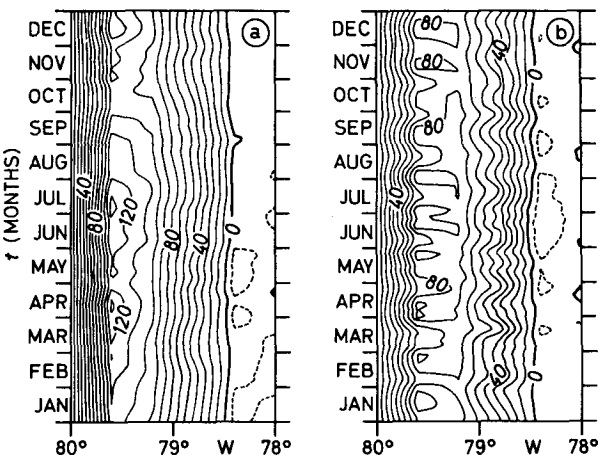

FIG. 6. Phase diagrams showing the meridional velocity component in the Florida Straits as a function of longitude and time, at 27°N. (a) Surface velocity for the experiment (KIEL 2) with Isemer–Hasse forcing, and (b) for the experiment (KIEL 3) with the same forcing, but reduced horizontal friction.

The most prominent feature of linear wind-driven models (AC, GG) in the region to the east of the Bahama Bank is the strong annual variation with a maximum northward flow in January, and a minimum in October. The phase diagrams of the velocity anomaly, $v' = v - \bar{v}$ (Fig. 7), give no indication of an annual cycle of this kind. Both the upper and the lower layer are dominated by fluctuations with periods of 80–120 days. Away from the continental slope we find a westward-propagating wave signal with phase speeds of 3–5 cm s^{-1}, indicative of baroclinic Rossby waves. The intensity of the fluctuations increases to the west; the signal is strongest at 75.6°W, with velocity anomalies in the 232 m level, between +30 and −40 cm s^{-1}. The core speed v of the Antilles Current, at 76°W, pulsates between 0 and 45 cm s^{-1}; the DWBC between −4 and −20 cm s^{-1}.

The fluctuations are not caused by the seasonal wind forcing: they similarly appear in experiment 2A where we applied a constant wind forcing. The intensity of the fluctuations is sensitive to the horizontal friction. Maximum values of eddy kinetic energy (EKE) are found at about 27.5°N with 300 $cm^2\ s^{-2}$ in 300 m, in the case of experiment KIEL 2 (Fig. 8). When the smaller friction coefficients are used (KIEL 3), EKE increases to more than 400 $cm^2\ s^{-2}$ in this region. The horizontal distribution of EKE suggests a local cause of the fluctuations. In particular, the region of high EKE associated with the Gulf Stream recirculation is separated from the eddy field east of the Bahamas by an area of weak eddy intensity at ~29°N.

Figure 9 shows a zonal section of EKE at 26.5°N, together with the kinetic energy of the mean flow (KEM). The Antilles Current and the DWBC stand out as distinct cores of high KEM near the continental slope. The distribution of EKE appears closely related to the mean flow pattern, both vertically and horizontally (Fig. 8), suggestive of a local instability mechanism. Highest EKE values (180 $cm^2\ s^{-2}$) occur in a subsurface core to the northeast of the KEM maximum, i.e., in the region of high lateral mean shear. The EKE values in the model are similar to the values (>150 $cm^2\ s^{-2}$) found by Lee et al. (1990) and Rosenfeld et al. (1989) near the core of the Antilles Current. The deep EKE values in the model (14 $cm^2\ s^{-2}$ at 2000 m) are smaller than the observed values (75 $cm^2\ s^{-2}$) in the proximity of the DWBC core. This may be related to the weaker DWBC in the model. The model gives larger values at the DWBC level, for both KEM (85 $cm^2\ s^{-2}$) and EKE (55 $cm^2\ s^{-2}$), in the region north of Haiti. In that region the deep values of EKE are even stronger than the subsurface maximum (~15 $cm^2\ s^{-2}$) associated with the Antilles Current. This suggests that the intensity of the deep fluctuations is related to the local intensity of the mean flow.

A source of eddy kinetic energy can be provided by the work of the Reynolds stresses against the mean shear (barotropic instability). In the equation governing the time rate of change of EKE,

$$\frac{1}{2}\frac{d}{dt}(\overline{u'^2 + v'^2}),$$

the Reynolds interaction term is given by

$$-\overline{u'u'}\frac{\partial \bar{u}}{\partial x} - \overline{v'v'}\frac{\partial \bar{v}}{\partial y} - \overline{u'v'}\frac{\partial \bar{v}}{\partial x} - \overline{u'v'}\frac{\partial \bar{u}}{\partial y}.$$

The distribution of the Reynolds interaction work at 27°N is characterized by a distinct maximum at the same depth and longitude as the maximum eddy kinetic energy, indicating barotropic instability of the Antilles Current as a major source of the velocity fluctuations in this area (Fig. 10). The largest contribution to the energy transfer comes from the interaction between the meridional velocity fluctuations and the downstream variation of the mean northward flow, $-\overline{v'v'}(\partial \bar{v}/\partial y)$. As in the observations, eddy kinetic energy near the current core is dominated by $\overline{v'^2}$, whereas the fluctuations become more isotropic away from the energy maximum.

4. The seasonal cycle of the Florida Current

a. Sensitivity to wind forcing

Figure 11a shows the annual cycles of the transport through Florida Straits of the experiments with HR forcing (KIEL 1) and with IH forcing (KIEL 2). Though monthly mean forcing fields are applied, the model response contains flow variability from synoptic eddies to interannual variability. The curves give the annual cycles as obtained by averaging over five model years; the stippling indicates the standard deviation from the mean value.

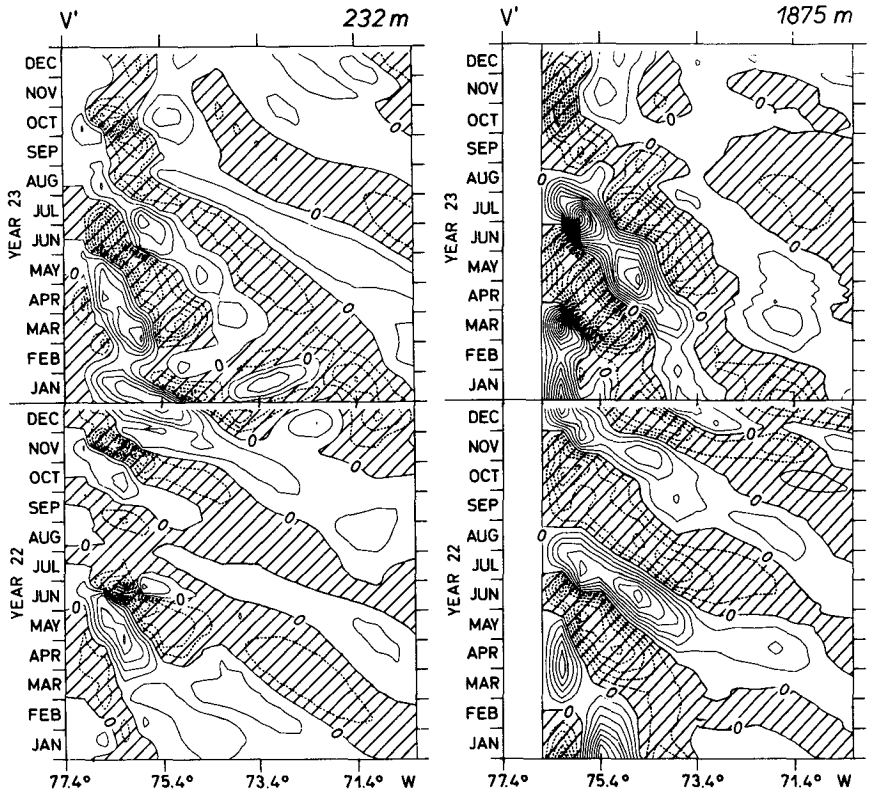

FIG. 7. Phase diagrams showing the anomaly of the meridional velocity component, $v - \bar{v}$, as a function of longitude and time, for a section to the east of the Bahamas at 27°N. (a) Model level 6 (232 m), contour interval 5 cm s^{-1}; (b) level 16 (1875 m), contour interval 1 cm s^{-1}.

The annual mean transport predicted by the model is 23.2 Sv with HR forcing. The annual range is about 3.4 Sv. It is interesting to note that in this case the variation of the transport about the annual mean is indistinguishable from the transport anomalies as obtained by the more idealized models of AC and GG (Fig. 11b); a similar variation is also obtained by SBB. All these models are forced by HR; they include, in a

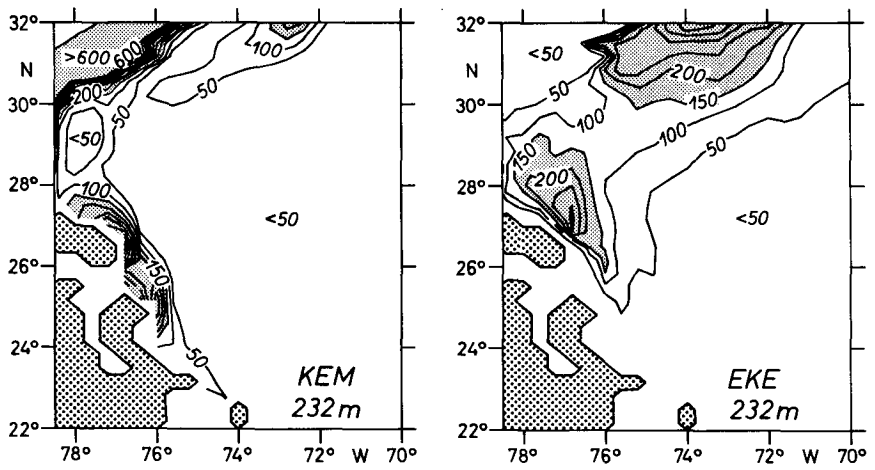

FIG. 8. Horizontal maps of the kinetic energy of the mean flow (KEM) and of the mean eddy kinetic energy (EKE) in 232-m depth. The contour interval is 50 cm s^{-2}, areas with >150 cm^2 s^{-2} are stippled. Experiment KIEL 2.

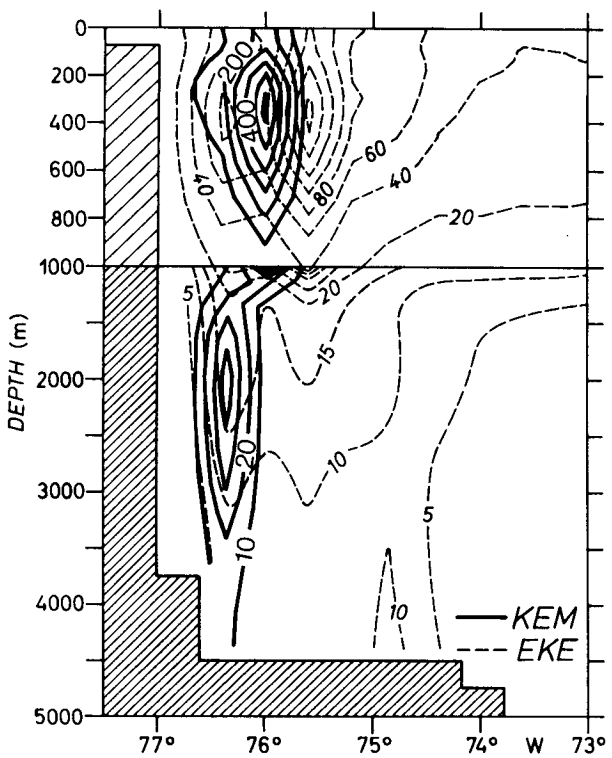

FIG. 9. Zonal sections at 26°N showing the kinetic energy of the mean flow (KEM) and the mean eddy kinetic energy (EKE), for experiment KIEL 2. Contour intervals above 1000 m are 20 cm^2 s^{-2} for EKE, and 100 cm^2 s^{-2} for KEM, below 1000 m, 5 and 10 cm^2 s^{-2}, respectively.

smoothed way, the large-scale bottom topography of the North Atlantic, but strongly differ in many details of the model representation of islands and passages.

As noted in the Introduction, the models are able to reproduce the observed phase of the seasonal cycle, but underestimate the amplitude by roughly a factor of 2. The differences between the transport anomalies of these completely different model configurations are much smaller than the change obtained by using the new wind-stress climatology of IH (Fig. 11a). Both the annual mean transport and the amplitude of the annual cycle significantly increase when the model is forced by IH: the model then gives a mean of 29.1 Sv and an annual range of 6.3 Sv, nearly twice the value obtained with HR forcing. It seems that the model is in much better agreement with the observational evidence (e.g., Schott et al. 1988; Molinari et al. 1990), both with respect to the annual mean and annual range.

It was found by AC that the seasonal variation of the Florida Current was not significantly different between the first and third model year. We see a similar behavior in the present model: the annual variation adjusts to its new equilibrium within the first year after the switch to the new wind forcing function. A similar adjustment time scale cannot be expected, however, for the annual mean transport. The question whether the mean transport continues to change slowly by baroclinic adjustment processes was addressed by an extension of experiment 2 over three more years. The annual mean values of transport for all eight model years with IH forcing are (in Sv): 28.2, 30.7, 28.8, 29.2, 28.3, 28.4, 29.9, 29.9. Apparently, there is some random interannual variation but no clear indication of a mean trend. The transport over the first 4 years with IH forcing (29.2 Sv) is not significantly different from the mean value we obtain from the last 4 years (29.1 Sv).

Since, in the present model, the contribution to the Florida Current by flow through passages in the Bahamas is very weak (<0.1 Sv), the transport through the Florida Straits is nearly identical to the transport through the Yucatan Strait and, thus, given by the sum of the inflow through the Antilles passages. The contribution to the mean transport of the Florida Current (29.1 Sv) is 6.5 Sv by Windward Passage, 10.6 Sv by Mona and Anegada, and 12 Sv by flow through the

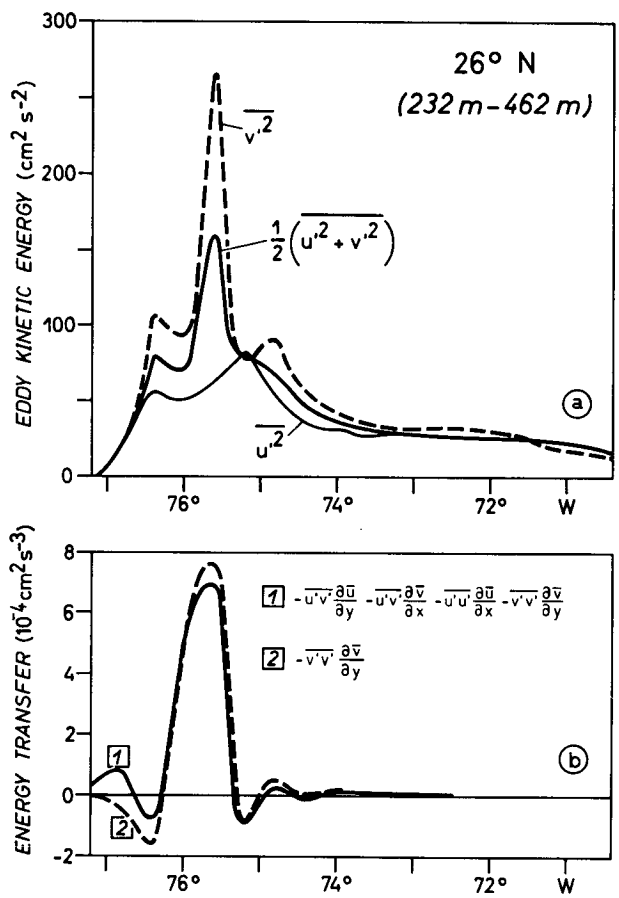

FIG. 10. (a) Zonal distribution of zonal velocity variance, $\overline{u'u'}$, meridional velocity variance, $\overline{v'v'}$, and eddy kinetic energy (EKE), $\frac{1}{2}(\overline{u'u'} + \overline{v'v'})$ at 26°N, averaged between levels 6 and 9 (232 to 462 m). Experiment KIEL 3. (b) Zonal distribution of total Reynolds interaction work (1), and the contribution of $\overline{v'v'}(\partial\bar{v}/\partial y)$ (2), for the same section as in (a).

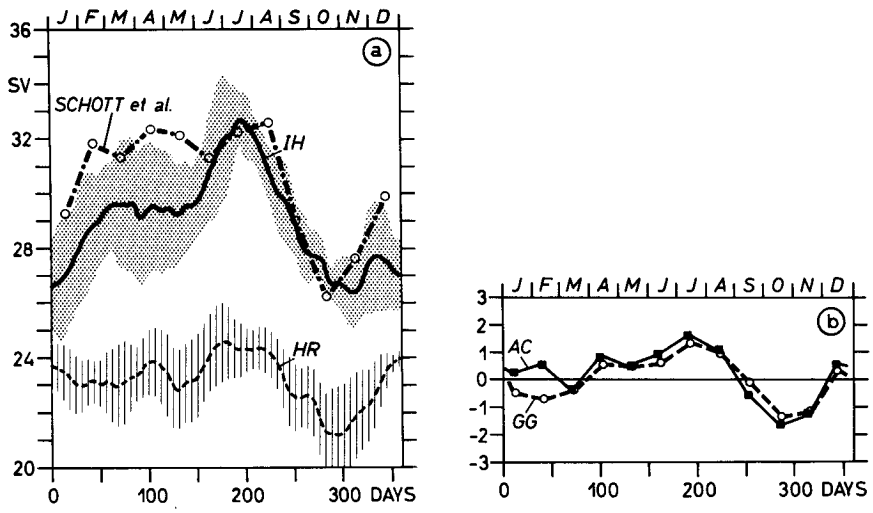

FIG. 11. (a) The annual cycle of the volume transport through Florida Straits from 5 years of model integration with HR forcing and IH forcing, respectively. The stippling indicates the standard deviation from the 5-year mean cycle due to eddy activity and interannual variability. The dash-dotted line indicates the observed monthly transports from Schott et al. (1988). (b) Monthly transport anomalies of the Florida Current as seen in the linear numerical models of Anderson and Corry (1985b), denoted AC, and Greatbatch and Goulding (1989), denoted GG.

passages of the Lesser Antilles. Figure 12 shows the mean annual cycles of the transport through the "northern" passages (Windward, Mona, Anegada, and the passage between Guadaloupe and Martinique), and the "southern" passages (south of Martinique), for the case of IH forcing. A summer maximum in transport is visible only in the southern passages (south of Martinique). The difference in net transport between HR and IH forcing is associated with the inflow through the northern passages, whereas the annual variation of the inflow south of Martinique appears mainly unaffected.

The annual mean southward Sverdrup transport of the subtropical gyre at 26°N (when integrating the Sverdrup relation from the African coast to 76°W) is 23.9 Sv for HR, and 35.6 Sv for IH. These values indicate that, in the present model, the mean northward transport of the Florida Current is not sufficient to close the wind-driven gyre. At a first sight, this appears to be different from the results of previous models. With a barotropic version of their model, AC obtained a mean transport of 30.5 Sv in the Florida Straits, driven by the annual mean HR stress. However, only 22.5 Sv of that is contributed by flow through the Yucatan Straits, very similar to the value given by the present model (23.2 Sv); the difference is due to a high transport (8 Sv) in the AC model through passages between Cuba and the Bahamas, which could be a result of the particular configuration of islands and topography in their coarse-resolution model. As noted above, transport through passages in the Bahamas is very weak in the present model. We will return to the question of an overall transport balance in section 6.

b. *Influence of various forcing regions*

While the enhancement of the annual mean transport in the case of IH forcing can be understood as an implication of the stronger trades and, consequently, stronger Sverdrup transports in the subtropical North

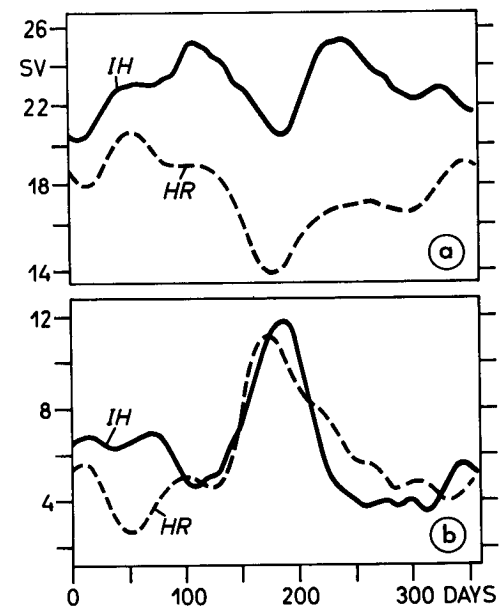

FIG. 12. The annual cycle of the volume transport entering the Caribbean Sea through the passages between Cuba and Martinique (a) and the passages south of Martinique (b). The Florida Straits transport is given, within 0.1 Sv, by the sum of the passage transports in (a) and (b).

Atlantic, an explanation of the enhanced annual variation is not as obvious. Clearly the larger annual range of the transport has to be associated with a larger annual range of the forcing function. This naturally leads to the related question: Where is the relevant forcing region for the particular seasonal cycle of the Florida Current? In this section the question of the forcing region will be addressed in two steps: we shall begin with a discussion of some sensitivity experiments (2A–D), which indicate the importance of wind forcing over the western North Atlantic sector between the Caribbean Sea and about the latitude of Cape Hatteras. The range of possible forcing regions will be narrowed then by comparing the amplitudes and phases of the HR and IH wind-stress fields over that area.

A first perspective of the forcing region for the seasonal variation of the Florida Current is provided by a series of experiments in which the seasonality of the wind stress was eliminated in certain regions. All experiments were initialized at year 20.0. In a first step (2A), the wind was held constant over the whole model domain, i.e., we kept the January wind for the integration. In the subsequent experiments this procedure was repeated by keeping the wind stress constant only in certain regions: first, for the North Atlantic north of 35°N (2B); second, in the Caribbean Sea and western North Atlantic (west of 60°W and south of 30°N) (2C), and finally in the equatorial region south of 10°N (2D). In all cases with regionally constant wind forcing, buffer zones of 5° width were applied around these regions in which the January winds were linearly merged with the seasonal winds of the adjacent regions.

Changing the forcing in the equatorial region (2D) had a strong effect on the seasonality of the equatorial current system (e.g., the North Equatorial Counter Current vanishes), but influences on the transport variation farther north were negligible. Time series of transport through the Florida Straits for the other experiments are shown in Fig. 13. Two effects can be distinguished here: the mean transport adjusts to a new equilibrium value, and the amplitude of the seasonal cycle is reduced. Both effects depend on the relative importance of the respective forcing region. In cases A and C the mean transport through the straits is enhanced as a consequence of the fact that the January wind-stress curl in the subtropical North Atlantic is larger than the annual mean value of the curl. The time scale of this response is O(1/2 year). Thus, the adjustment takes much longer than the barotropic time scale; on the other hand, the response is faster than a baroclinic adjustment to processes in the central Atlantic, which points at the importance of forcing in the west. The mean transport of ~29 Sv obtained with seasonal IH forcing (2) increases to ~34 Sv when the January stresses are applied everywhere (2A). A substantial fraction of the additional transport is provided by forcing over the Caribbean/western Atlantic sector: the transport already increases to ~32 Sv when the

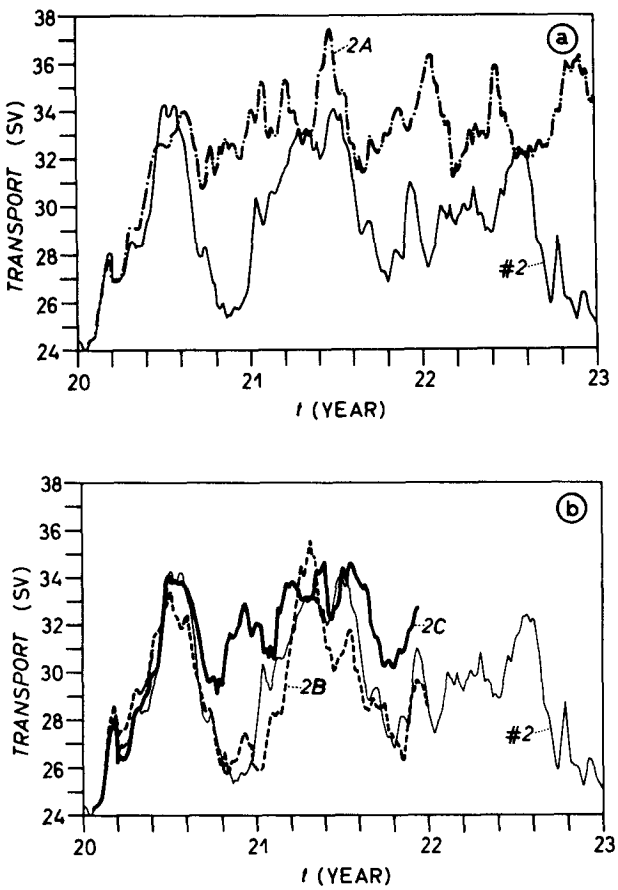

FIG. 13. Time series of volume transport through the Florida Straits for the sensitivity experiments with regionally constant wind forcing. Experiments were started at year 20.0. In case 2A the wind was held constant (at its January value) over the whole model domain, in case 2C only over the Caribbean/western subtropical Atlantic, and in 2B north of 35°N. Also indicated is the reference solution of KIEL 2, with seasonal IH forcing over the whole model domain.

January winds are applied in this region only (2C). In contrast, the contribution from forcing north of 35°N is much smaller; the January winds applied there (2B) have only a negligible influence on the mean transport.

The time series are rather short to quantitatively extract the effect of the forcing regions on the amplitude of the seasonal signal. In 2A the seasonal cycle apparently vanishes but the transport continues to oscillate between 32 and 36 Sv, on a shorter time scale. We do not have an explanation for the nature of these oscillations. Obviously the possible contamination of the transport variation in 2B and 2C by these random fluctuations prevents a quantitative interpretation of the seasonal cycle. It is clear, however, that the influence of the northern regions on the seasonal variation in the straits appears much smaller than the influence of forcing over the Caribbean/Florida Straits area: eliminating the seasonal forcing north of 35°N (2B) has a negligible effect on the amplitude of the transport vari-

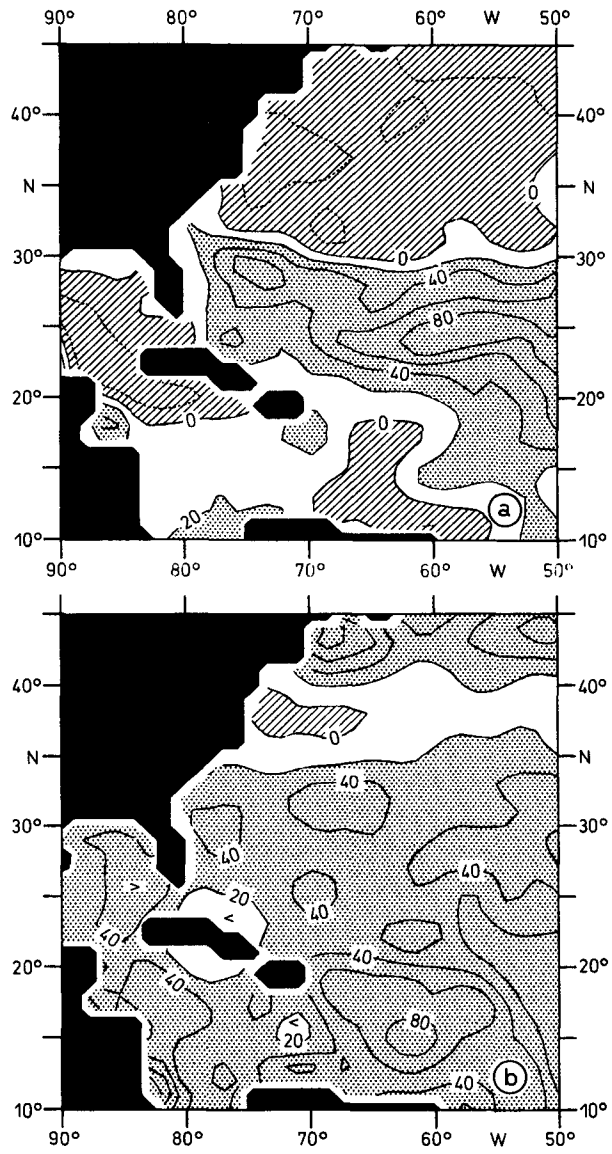

FIG. 14. The percentage deviation of the annual range of the wind stress given by the IH climatology from the annual range given by the HR climatology, (a) for $|\vec{\tau}|$; hatching indicates areas with negative values, i.e., larger annual amplitudes of the HR stresses, stippling denotes differences of more than 20%; (b) for τ^y.

ation, whereas the amplitude appears significantly reduced in 2C.

Maps of the differences between IH and HR of the annual ranges of $|\vec{\tau}|$ and $\tau^{(y)}$ are displayed, for the western North Atlantic and the Caribbean Sea, in Fig. 14. The annual variation of the wind stress $|\vec{\tau}|$ mainly increases in the latitude belt of about 20°–30°N. In the western North Atlantic this is mainly due to an enhanced amplitude of $\tau^{(y)}$. The forcing by the meridional component of the stress was identified by AC to provide the major contribution to the seasonal cycle in their model: They showed that transport can be generated by wind stress over varying topography and by the passage of coastally trapped waves excited to the north of the straits. Since north of 32°–35°N the amplitudes of the stress components given in IH are smaller than the corresponding amplitudes in HR, there can be no contribution from these regions to the enhanced annual variation of transport obtained with IH forcing.

The time dependence of $\tau^{(y)}$ in the Florida Straits (26°N) and north of it (30°N) is shown in Fig. 15. As has been noted earlier by Schott et al. (1988), the phase of the annual variation, with a maximum northward stress in July and a minimum in October, closely resembles the phase of the Florida Current. Lee and Williams (1988) concluded from the results of a simple wind-forced channel model that the local along-channel winds could provide a significant contribution to the seasonal changes of the transport. The different annual amplitudes seen in our model solutions obtained with HR and IH forcing (Fig. 11) appear to be consistent with this possibility. The seasonal differences in the meridional stress component are substantially en-

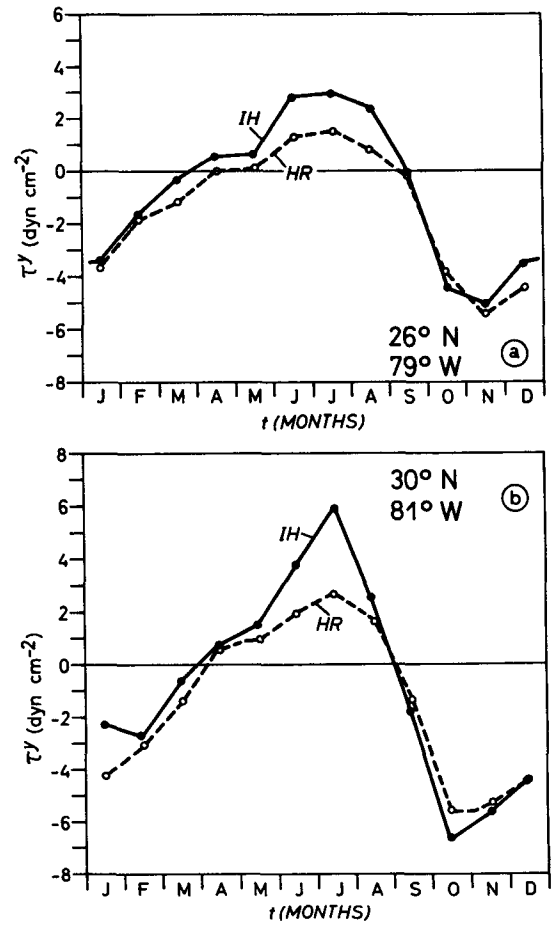

FIG. 15. The meridional stress component τ^y as a function of time; (a) in the Florida Straits, 26°N; (b) north of the Straits, at 30°N.

hanced in the IH climatology. A similar phase and a similar tendency between HR and IH can be found for the meridional stress over the Yucatan Straits. In contrast, we see no substantial difference between the amplitudes of the zonal stresses of IH and HR over the channel between Cuba and Florida, which also show a similar phase as the transport through the straits (Schott et al. 1988).

Another possible generation mechanism for the transport cycle was proposed by Schott and Zantopp (1985), who noted the same type of seasonality in the negative wind-stress curl over the western Caribbean. An inspection of the monthly values of curl obtained from the HR and IH stresses indicates, however, that there are strong local differences between the seasonality of the wind-stress curl. We find a seasonal cycle of the type shown by Schott and Zantopp (1985) only over the Yucatan Basin and over parts of the Gulf of Mexico; only in the latter region there is a larger annual amplitude in IH. The seasonalities are very different over the Colombian and the Venezuelan basins. Therefore, an examination of the wind-stress fields yields no evidence for an influence of wind forcing over the Caribbean Sea to the seasonal variation of the Florida Current. This is consistent with a model result of AC. Applying wind stress to the Caribbean Sea only, they obtained (with a homogeneous version of their model) a transport variation of only ±0.5 Sv. After excluding the Caribbean Sea as a major contributor, the combined evidence from the model results and the structure of the wind-stress fields suggest that the seasonal variation of the Florida Current is mainly forced by the meridional component of the stress in the vicinity of the straits.

c. Sensitivity to horizontal friction

In experiments with an idealized, homogeneous model by Anderson and Corry (1985a) the transport between the western boundary and an island near this boundary appeared systematically dependent on the magnitude of the model friction. When the model was forced by wind stress in the interior, the bulk of the boundary current was caught to the east of the island, and the proportion of the transport passing west of the island increased with increasing friction. A different frictional effect was found in the homogeneous model of GG, using realistic geometry, but no islands. In their model, the boundary current transport increased with decreasing friction. Apparently, the influence of friction can depend in a delicate way on details of the basin and forcing geometries and, perhaps, on model resolution.

It is computationally not feasible to use the present model for a thorough study of parameter sensitivity. However, the tendency of the frictional influence on the Florida Current in the model may be seen from our experiment (KIEL 3) with reduced lateral friction coefficients.

Reducing lateral friction leads to an enhanced shear instability of the Florida Current (Fig. 6). Maximum velocities decrease, and the previously almost laminar flow obtains a more turbulent character. The high-frequency variability of the current implies transport fluctuations of ±1–2 Sv (Fig. 16). The mean transport (averaged over four model years) substantially decreases, from 29.1 to 25.5 Sv. Associated with this decrease of Florida Straits transport is a similar decrease of the transport through Windward Passage (from 6.5 Sv down to 1.9 Sv), whereas the inflow through all other Caribbean passages is nearly unaffected.

5. Transport variation east of Bahama

As exhibited by the phase diagrams (Fig. 7), both the Antilles Current and the DWBC are subject to strong temporal oscillations. Time series of one model year (KIEL 3) of the meridional volume transport through sections at 26°N, east of the Bahama Bank, are shown in Fig. 17. The transport variations depend on the zonal width of the section. In the narrower section, between 77° and 75.4°W, there are strong fluctuations, of similar phase and amplitude in the upper (0–1000 m) and lower layers (1000 m–bottom), with a time scale of about 100 days. The vertically integrated transport varies between +30 and −18 Sv. There is no indication of an annual signal in this record. Moving the eastern boundary of the cross section to 73°W has a substantial effect on the transport variation. The fluctuations appear much smaller over this wider section, indicating that a large fraction of the current anomalies are compensated by a local recirculation east of the current axis.

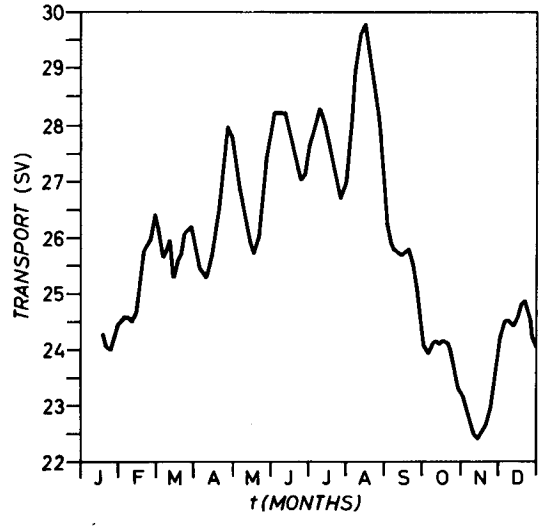

FIG. 16. Time series of Florida Straits transport, over one model year, for experiment KIEL 3 with reduced horizontal friction.

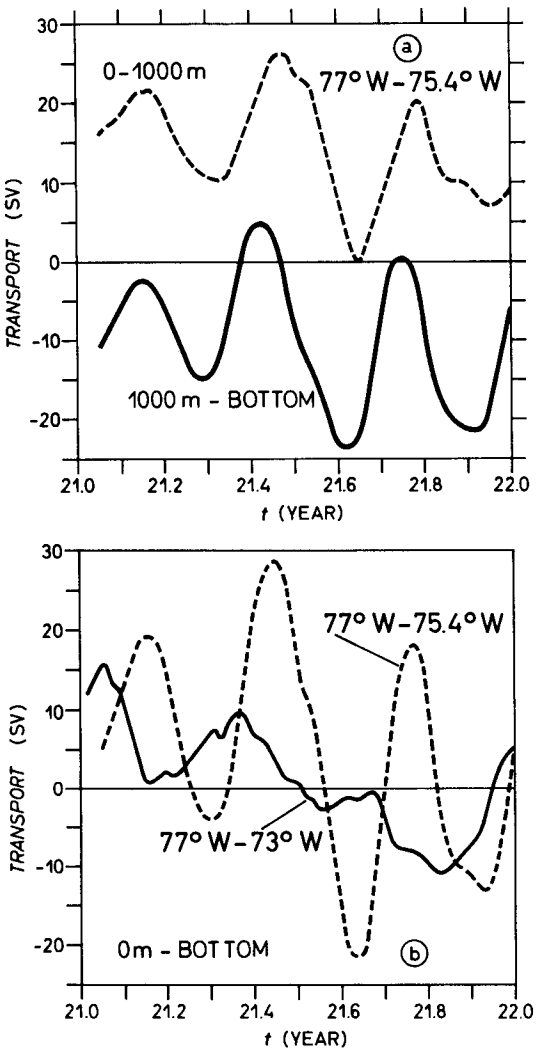

FIG. 17. Meridional volume transport, over one model year of experiment KIEL 3, through a zonal section east of the Bahama Bank, at 26°N. (a) Upper- and lower-layer transports, between 77° and 75.4°W. (b) Vertically integrated transports for two different widths of the section.

Figure 18a shows time series of the total transport for four consecutive years, between 80° and 74°W, i.e., a cross section that encompasses the Florida Current, the Antilles Current, and the DWBC. The variability of the boundary current system as a whole is dominated by the oscillations east of the Bahamas. Strong deviations between individual years suggest a partly stochastic character of these oscillations. Averaging over 4 years certainly cannot provide a stable mean annual cycle. Nevertheless, the mean cycle in Fig. 18b shows a remarkable tendency toward the annual variation obtained in previous, non-eddy–resolving models (AC, GG). Transport anomalies are about ±(10 to 15) Sv, with a minimum northward transport in fall, a maximum in winter, and a secondary maximum in summer. The contribution from the deeper layer (1000 m–bottom) is about three times larger than the contribution from the layer above, consistent with a largely barotropic nature of the annual signal.

A similar seasonal variation is also obtained with a non-eddy–resolving version (zonal grid spacing 1.2°, meridional grid spacing 1°) of the present model. Figure 19 shows the annual cycle of the western boundary current transport after 20 years of integration with the

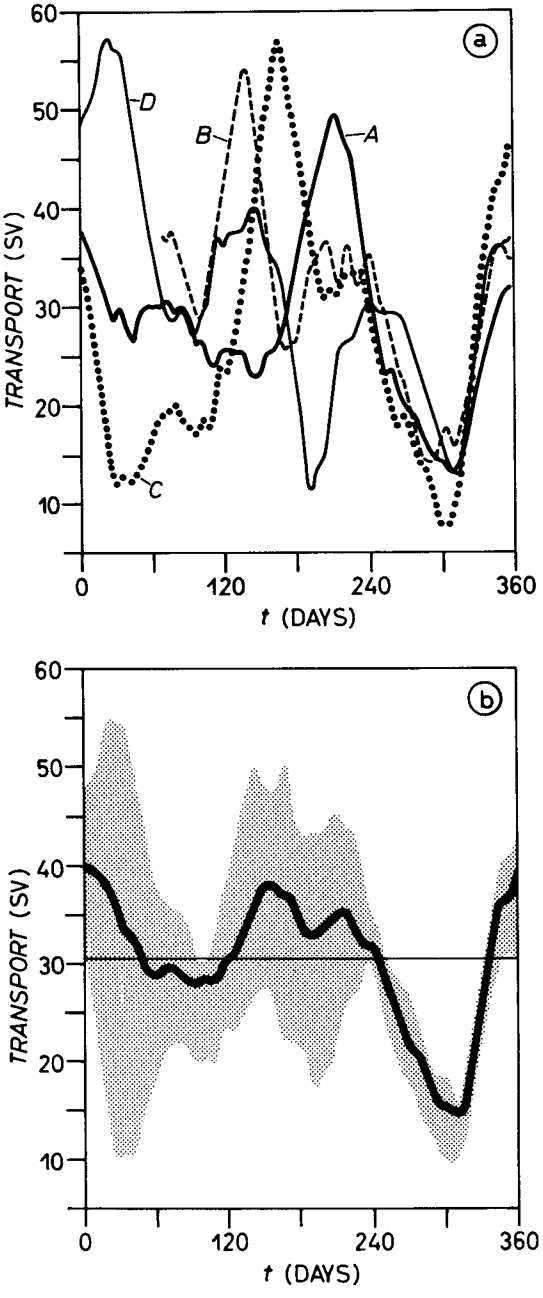

FIG. 18. Meridional volume transport at 26°N, between 80° and 74°W, for four individual model years (A–D) (a), and averaged over these 4 years (b); Experiment KIEL 3.

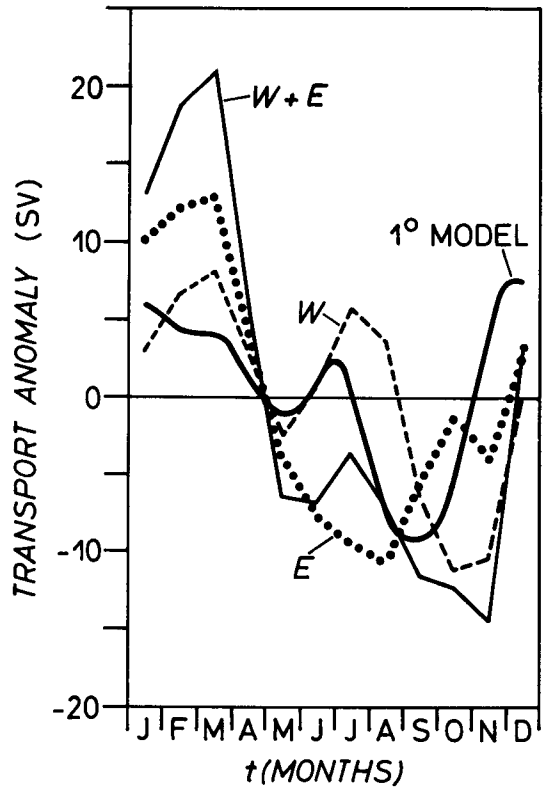

FIG. 19. Monthly values of the negative Sverdrup transport streamfunction obtained from integrating $-\text{curl}\vec{\tau}/\beta$, at 26°N, between the African coast and 46°W (E), between 46° and 78°W (W), and over the whole width of the basin (W + E). Also displayed is the transport of the western boundary current, between Florida and 78°W, obtained with a coarser version (1° resolution) of the circulation model, forced with IH stresses over 20 years.

IH stresses. The transport anomalies are roughly in phase with the wind-stress curl at this latitude. More specifically, the Sverdrup transports obtained by integrating $\text{curl}\vec{\tau}/\beta$ over different fractions of the zonal section at 26°N suggest that the seasonal transport anomalies seen at the western boundary are forced mainly in the western part of the Atlantic basin. In the eastern basin $\text{curl}\vec{\tau}$ is clearly dominated by an annual variation. The origin of the summer maximum in transport is in the western part of the basin where $\text{curl}\vec{\tau}$ shows a distinct semiannual variation. In contrast, the annual mean transport in the model (see section 6) resembles the Sverdrup transport obtained from integrating over the whole basin.

6. Mean transport balance at 26°N

Integrating the Sverdrup relation between the African coast and 76°W predicts a wind-driven southward transport of 23.9 Sv when using the HR stresses and 35.6 Sv when using IH. With HR forcing (KIEL 1) the model gives an annual mean Florida Straits transport of 23.2 Sv, with IH forcing (KIEL 2) 29.1 Sv. How does the mean northward transport of the boundary current system correspond to the thermohaline and wind-driven southward transport in the interior of the ocean? And how does the interior transport correspond to the transport predicted by the Sverdrup balance? A schematic of the mean transport balance at 26°N is displayed in Fig. 20. The transport values represent averages over the last 4 years of the 8-year integration period with the IH stresses (KIEL 2). In addition, the mean, upper-layer transport of the model forced with the HR stresses (KIEL 1) are indicated in parentheses. Differences between the model transports are relatively small in the deeper layer, i.e., smaller than the year-to-year variation of these values.

Due to the nonlinear character of the problem, a separation of the transport into a thermohaline and a wind-driven part is, in principle, not possible. However, it is interesting to note that both values for the mean southward transport in the upper 1000 m, east of 76°W, closely resemble the respective values given by the Sverdrup relation: 34.9 Sv with IH and 25.0 Sv with HR. The southward transport of the DWBC is partially compensated by northward flow in the deep ocean interior. The net southward transport below 1000 m is 6–7 Sv. The value of the deep transport appears significantly smaller than the estimates from hydrographic data mentioned in the Introduction, indicating a serious model deficiency with respect to the strength of the thermohaline circulation.

The combined southward transport of the upper-layer, interior "wind-driven" flow and the deep "thermohaline" flow is balanced by the Florida Current and the Antilles Current. The additional 9 Sv of interior southward transport obtained with IH forcing are mainly balanced by an increased Florida Current (+6 Sv). One should expect that the partition of the northward transport into parts to the west and to the east of the Bahamas is sensitive to details of the model formulation, i.e., the model friction and the representation of islands and passages. However, the total northward transport of the boundary current system should be a rather stable function of the interior forcing. With IH forcing this value, 41.1 Sv appears rather large when compared with the existing observational evidence for the Florida Current (29–32 Sv) and the estimates for the Antilles Current (3–5 Sv). Together with the fact that the thermohaline part of the circulation seems too weak, this would indicate that the mean wind-driven circulation in the subtropics is too strong in this solution.

In this respect it should be noted that some of the section transports displayed in Fig. 20 show strong year-to-year variations. This is especially the case for the Antilles Current (yearly averages, for IH forcing, vary between 9 and 18 Sv) and the upper-layer interior flow (between −30 and −39 Sv), and, to a lesser extent, also for the DWBC (between −7 and −9 Sv); the annual mean transport of the Florida Current appears

more stable with variations of less than ±1 Sv. Additional variability could be expected from the interannual variability of the real winds, which is neglected in the present experiments. Thus given the strong transport fluctuations of the Antilles Current/DWBC (Lee et al. 1990), and the possibility of an interannual variability as indicated by the model, it seems that rather long time series of measurements would be necessary to establish a stable picture of the mean transport balance in the subtropical North Atlantic.

7. Annual cycle of meridional heat transport

We will now consider the meridional heat transport through the zonal cross section at 26°N. The annual cycle of heat transport through 26.5°N in the North Atlantic was recently estimated by Molinari et al. (1990) using the approach of Hall and Bryden (1982). Integrated across the basin, the net volume transport is zero and the heat transport, Q, is given by the covariance of meridional velocity v and potential temperature θ,

$$Q = \rho_0 c_p \int_0^L \int_0^{H(x)} v\theta dz dx, \qquad (1)$$

where ρ_0 denotes the mean density and c_p the specific heat for constant pressure. An additional contribution from the model diffusivity is so small that it can be neglected here. If, following Bryan (1962), v and θ are decomposed into depth-averaged ($[v]$, $[\theta]$) and depth-dependent (v^*, θ^*) components, Q can be written as

$$Q = Q_{BT} + Q_{BC} + Q_{EK} \qquad (2)$$

with

$$Q_{BT} = \rho_0 c_p \iint [v][\theta] dz dx$$

$$Q_{BC} = \rho_0 c_p \iint v^*\theta^* dz dx - Q_{EK}$$

$$Q_{EK} = \rho_0 c_p \left[\int \left(-\frac{\tau_x}{f} \theta^*_{surface} \right) dx \right] \Delta z_{surface} \qquad (3)$$

where $\Delta z_{surface}$ represents the vertical extent (35 m) of the uppermost grid box. We will refer to the heat transport due to the depth-averaged components of v and θ as the "barotropic" (Q_{BT}) and that due to the depth-dependent components of v and θ, minus the Ekman term (θ_{EK}), as the "baroclinic" (Q_{BC}) component of total heat transport.

The annual-mean heat transport at 26°N obtained with the present model is 0.64 PW (0.66 PW) in the case of IH (HR) forcing. These model values are much lower than most estimates from oceanographic data, which tend to be in the range 1.0–1.2 PW (a list of recent computations is given in Molinari et al. 1990). The mean value can be considered as a contribution mainly from the thermohaline mode of the circulation, which, in the present model, is strongly constrained by

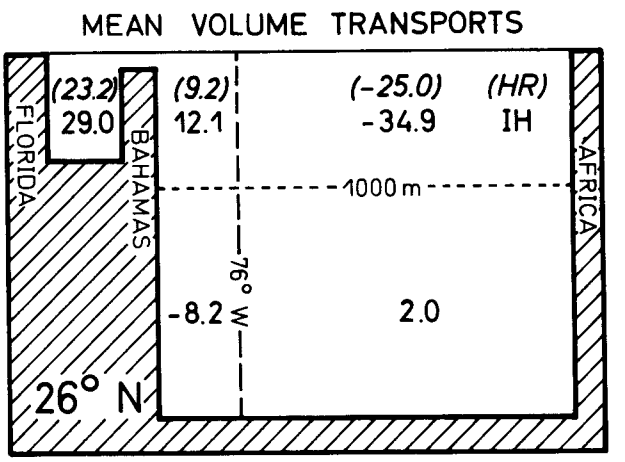

FIG. 20. Schematic representation of mean northward volume transports (in Sv) through various portions of a transatlantic section at 26°N. Values are obtained as averages over the last four model years (24.0 to 28.0) of the model experiment with IH forcing (KIEL 2). The upper-layer transports of the model with HR forcing (KIEL 1) are given in parentheses. For comparison, the wind-driven transports as predicted by the Sverdrup relation are −35.6 Sv (IH) and −23.9 Sv (HR) at this latitude between Africa and 76°W.

the choice of boundary conditions, particularly at the southern wall. The buffer zone near the boundary where a Newtonian damping of T and S toward the Levitus climatology is applied seems too narrow (5 grid boxes, or 1.67°) for effectively converting the cold, deep NADW to warm upper-layer waters. Parallel experiments with a coarser version of the present model show that the meridional overturning is enhanced significantly when the width of the buffer zone is increased to 5°. Sarmiento (1986) used a 10° wide buffer zone (between 30°S and 20°S) and obtained, at 25°N, a maximum value of transport in the meridional cell of 12.8 Sv, and a mean northward heat transport of 0.86 PW. In the following, we will focus on the seasonal deviations from the annual mean value.

Figure 21 shows the anomalies of the heat transport through 26°N as obtained with HR forcing (KIEL 1) and IH forcing (KIEL 2), in comparison with the estimates of Molinari et al. (1990). The shape of the annual cycle is similar to the volume transport through the Florida Straits, with a maximum in July–August. The strong role of the Florida Current on the seasonal cycle of heat transport is demonstrated also by the doubling of the annual range, from 0.44 PW with HR to 0.80 PW with IH forcing, consistent with the doubling of the annual range of the volume transport through the straits. The annual range obtained with HR forcing is similar to the model solution of Sarmiento (1986), which was forced by the same wind-stress climatology. The monthly heat transports computed by Molinari et al. show an annual range of 1.17 PW. Given the uncertainty (0.39 PW) of the observed monthly anomalies, this appears not significantly different from the model results obtained with IH forcing;

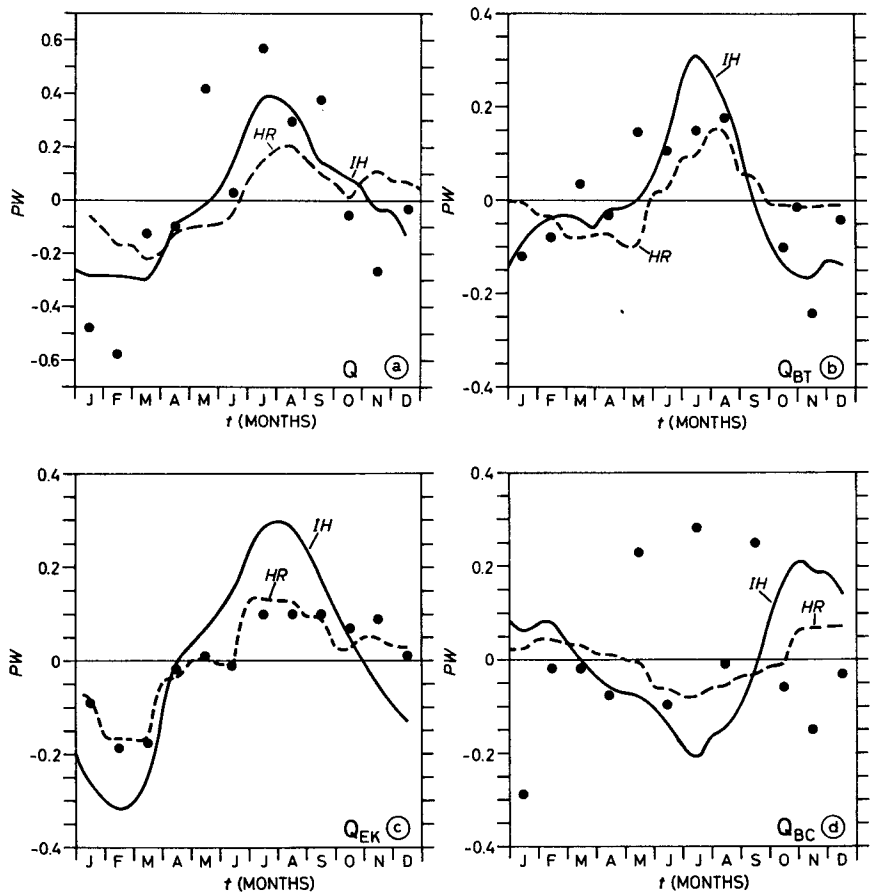

FIG. 21. Seasonal cycle of the zonally integrated northward heat transport at 26°N, obtained with HR and IH forcing (experiments KIEL 1 and 2), in comparison with observational estimates from Molinari et al. (1990) (dots). (a) Total heat transport Q, (b) the barotropic part Q_{BT}, (c) the Ekman part Q_{EK}, and (d) the baroclinic part Q_{BC}.

the observed annual range is more than twice, however, than in the model solutions forced with HR.

The strongest contribution to the observed seasonal variation of total heat transport is given by the barotropic component, Q_{BT}. As shown by Molinari et al., the barotropic term is dominated by the transport of the Florida Current times the temperature difference between the straits and the interior Atlantic. The observed annual range of Q_{BT} is ~0.4 PW; the model gives 0.24 PW with HR, and 0.50 PW with IH forcing. A similar phase as Q_{BT} is shown by the Ekman term, Q_{EK}. Since this term was computed by Molinari et al. by using the HR stresses and the surface temperatures as given by Levitus (1982), the model solution obtained with HR forcing must be similar to this. The annual range of Q_{EK} becomes twice as large with the IH stresses. The strongest discrepancy between model and observations appears in the baroclinic term, Q_{BC}. Whereas the observed seasonal cycle of Q_{BC} tends to reinforce the summer maximum of net northward heat transport, Q_{BC} in the model shows a reversed trend, with a maximum southward transport in summer. The increased annual range of Q_{EK} in the case of IH forcing is partially compensated by a similar tendency, but of opposite sign in the cycle of Q_{BC}.

8. Summary and conclusions

A high-resolution model of the wind-driven and thermohaline circulation was used to study the variability of the western boundary-current system in the subtropical North Atlantic. The model qualitatively reproduces the observed current structure west and east of the Bahamas; it also simulates the major modes of variability: the seasonal variation of the Florida Current, and the O(100 days) fluctuations of the Antilles Current and DWBC.

A serious deficiency is the apparent weakness of the thermohaline circulation and thereby of the mean meridional heat transport of the model. The maximum transport of the meridional overturning cell is about 12 Sv, at about 50°N; at 26°N the zonally integrated transport is 6–7 Sv, southward below 1100 m and northward above. The annual-mean heat transport at

this latitude is only 0.65 PW. This unsatisfactory feature of the model solutions appears related to the artificial way of closing the thermohaline cell near the southern boundary. Obviously, the dependence of the strength of the overturning cell on artificial model assumptions, an inherent problem of closed basin models, severely limits a quantitative examination of model features involving the mean thermohaline circulation. We assume that this limitation does not apply to the time-varying part of the circulation related to the seasonal wind forcing.

Probably the most interesting aspect of the model solutions concerning the seasonal variation of the Florida Current is the strong sensitivity to the wind-stress climatology. A strong feature of both the observations and the model solutions is the rapid drop from a (more or less broad) transport maximum in July–August to a distinct minimum in October–November. The annual range, i.e., the difference between the summer maximum and the fall minimum, has been used repeatedly (AC; GG; Leaman et al. 1987; Schott et al. 1988; Rosenfeld et al. 1989; Smith et al. 1990) for model–data comparisons. While previous models were able to reproduce the phase of the annual cycle, they consistently tended to underestimate the annual range.

The present high-resolution model forced with HR yielded virtually the same seasonal variation of the Florida Current as the earlier, much more idealized models of AC and GG, and it appears similar also to the solution of the isopycnic model of Smith et al. (1990). All these models include, though often in a heavily smoothed way, the large-scale bottom topography. They strongly differ, however, in many details of representation of islands and passages. The similarity of the model solutions, all forced by the HR stresses, indicate a rather robust nature of the seasonal cycle with respect to the model configuration. This also seems to hold with respect to the influence of model friction: the annual range did not change significantly between KIEL 2 and 3 (different horizontal friction), or between NCAR 1 (Bryan and Holland 1989) and KIEL 1 (different vertical viscosity).

Apparently, the amplitude of the seasonal variation is more sensitive to the wind forcing: the differences between the solutions of completely different models, forced by the same wind-stress climatology (HR), are much smaller than the change we obtained by using the new wind-stress climatology of IH; the annual range increases from 3.4 Sv with HR forcing to 6.3 Sv with IH forcing.

Together with the meteorological evidence of systematic errors in the drag coefficient formulation and in the Beaufort equivalents adopted by HR, the improved simulation of the observed transport indicates possible problems with the widely used HR stresses (Böning et al. 1990). However, the Florida Current cannot be seen in isolation. Though its mean transport is in better agreement with the observational evidence when the IH stresses are used (29.1 Sv vs 23.2 Sv with HR), the combined transport of the Florida and the Antilles currents appears rather high (>41 Sv). Observations east of the Bahamas led to estimates of a mean transport of 3–5 Sv by the Antilles Current (Olson et al. 1984; Lee et al. 1990). The mean velocity of the Antilles Current in the model shows similar maximum values (20–30 cm s^{-1}) as the observed one, but the transport that we get, above 1000 m, is much higher (9.3 Sv with HR and 12.1 Sv with IH). It still may be a question whether the observations east of Bahama, taken over rather short periods of time, are really representative. Rosenfeld et al. (1989) obtain a mean baroclinic transport of 12.2 Sv, above 1100 m, from velocity profiler sections taken over a period of 3 years.

It seems that the strong impact of the different wind-stress climatologies has to be regarded as a matter of critical importance to ocean modelers. Given the sensitivity of model solutions as demonstrated here, it appears important to recognize the uncertainties and the differences between existing wind-stress climatologies. In the past the similarity between the transport through the Florida Straits and the Sverdrup transport at this latitude had been used as a basis for regarding the Florida Current as the return flow of the wind-driven subtropical gyre (Leetma et al. 1977). Obviously such conclusions critically depend on the validity of the particular wind-stress field. The strong dependence of the Sverdrup transport on the wind-stress climatology under consideration, the contribution of the thermohaline circulation (Schmitz and Richardson 1990), and the participation of the Antilles Current in closing the transport balance complicate the situation considerably. It is interesting to note that the interior, upper-layer (0–1000 m) transport in both our model solutions, with HR and with IH forcing, appears in good agreement with the theoretical transport given by the Sverdrup balance. However only part of this wind-driven transport is returned by the Florida Current. We feel that a quantitative validation of the different model solutions appears almost impossible given the present uncertainty concerning the wind-stress fields and the range of estimates for important components of the WBC system, i.e., the mean transports of the Antilles Current and of the DWBC.

A puzzling feature of previous models (e.g., AC, GG) was the strong seasonal variation of the volume transport east of the Bahamas. That transport cycle, in phase with the negative Sverdrup transport at that latitude, constituted a robust model result, but appears in sharp contrast to observations (Olson et al. 1984; Lee et al. 1990), which gave no evidence of an annual signal. An explanation for the discrepancy is offered by the solutions of the high-resolution model used here. Time series of both observed (Lee et al. 1990) and model transports are dominated by strong fluctuations on shorter (about 100 days) time scales. The model shows that these oscillations effectively mask the weaker an-

nual variation. The residual signal, obtained after averaging over some model years (we used a 4-year period) is very similar to the seasonal cycle expected from the Sverdrup balance. This suggests that the apparent discrepancy between previous model solutions and observations east of Bahama simply occurs due to an incompatibility between coarse-resolution models, not capable of simulating instabilities of the boundary current, and observations, taken over periods of time that are too short to extract the annual signal from the strong random oscillations. It should be noted that the transport anomalies obtained by Rosenfeld et al. (1989), from 14 velocity profiler sections taken during a time interval of 3 years, are not inconsistent with the present model results. The observations indicate both a winter and a summer transport maximum, as we obtained in the case of IH forcing. This annual cycle can be explained as a barotropic response to the wind-stress curl over the western part of the basin.

Whereas the annual cycle in the deep ocean east of the Bahamas can be explained as a barotropic response to the wind-stress curl over the western part of the Atlantic basin, the seasonal variation of the Florida Current appears related to forcing in the vicinity of the straits. A contribution from wind stresses north of 32°–35°N can be ruled out for two reasons: first, the annual amplitude of the wind stress in the IH climatology is smaller there than the amplitude of the HR stress, and thus inconsistent with the enhanced annual transport variation obtained with IH forcing; second, elimination of the seasonal forcing there had little influence on the transport through the straits. From the results of our sensitivity experiments we are not able to separate the influence of forcing over the Caribbean Sea/Gulf of Mexico from local forcing in the straits. However, in contrast to the seasonal variation of the wind-stress curl over most of the Caribbean, the meridional stress in and just north of the straits shows the same phase *and* a larger annual amplitude in case of IH. The tendency of the forcing function points to the relevance of the latter region, whose possible role was suggested by Schott et al. (1988) and Lee and Williams (1988). An annual signal generated in the straits and over the Blake Plateau north of the straits could be communicated upstream by the coastally trapped waves envisioned by AC, thereby generating the transport variation in the passage between Martinique and South America.

Though the variation of the volume transport east of the Bahama Ridge is much larger than the seasonal cycle of the Florida Current; the latter has a stronger impact on the variation of the net meridional heat transport in the Atlantic Ocean at 26°N. Both the observational estimates of Molinari et al. (1990) and the model results show a seasonal cycle of heat transport that is in phase with the Florida Current. In the model, both the Ekman transport over the interior Atlantic and the barotropic term, related to the volume transport through the straits times the temperature difference between the straits and the interior Atlantic, contribute to the variation of the heat transport, whereas the phase of the baroclinic term is reverse. Again, the annual range seen in the observations (1.17 PW) is simulated better when the model is forced with the IH stresses (0.80 PW) than with HR (0.44 PW).

Acknowledgments. We thank F. Bryan and W. Holland for generously providing the model code and sharing their experience from the initial experiments of the Community Modeling Effort. We thank R. Gerdes and J. Kielmann for their efforts at improving the efficiency of the model computations at the CRAY X-MP of Kiel University, and M. Hamann for helping in the model evaluation. The study benefitted from helpful discussions with F. Schott. This work is supported by the Deutsche Forschungsgemeinschaft, Sonderforschungsbereich 133.

REFERENCES

Anderson, D. L. T., and P. D. Killworth, 1977: Spin-up of a stratified ocean, with topography. *Deep-Sea Res.*, **24**, 709–732.

——, and R. A. Corry, 1985a: Ocean response to low frequency wind forcing with application to the seasonal variation in the Florida Straits–Gulf Stream transport. *Progress in Oceanography*, Vol. 14, Pergamon, 7–40.

——, and ——, 1985b: Seasonal transport variation in the Florida Straits: A model study. *J. Phys. Oceanogr.*, **15**, 773–786.

——, K. Bryan, A. E. Gill and R. C. Pacanowski, 1979: The transient response of the North Atlantic: Some model studies. *J. Geophys. Res.*, **84**(C8), 4795–4815.

Böning, C. W., R. Döscher and H.-J. Isemer, 1991: Monthly mean wind stress and Sverdrup transports in the North Atlantic: A comparison of the Hellerman–Rosenstein and Isemer–Hasse climatologies. *J. Phys. Oceanogr.*, **21**, 221–235.

Bryan, K., 1962: Measurements of meridional heat transport by ocean currents. *J. Geophys. Res.*, **67**, 3403–3414.

——, 1969: A numerical method for the study of the circulation of the World Ocean. *J. Comput. Phys.*, **4**, 347–376.

Bryan, F. O., and W. R. Holland, 1989: A high-resolution simulation of the wind- and thermohaline driven circulation in the North Atlantic Ocean. *Parameterization of Small-Scale Processes. Proc. 'Aha Huliko'a, Hawaiian Winter Workshop*, P. Müller, D. Henderson, Eds., University of Hawaii at Manoa, 99–115.

Bunker, A. F., 1976: Computations of surface energy flux and annual air–sea interaction cycles of the North Atlantic Ocean. *Mon. Wea. Rev.*, **104**, 1127–1140.

Chelton, D. B., A. M. Mestas-Nunez and M. H. Freilich, 1990: Global wind stress and Sverdrup circulation from the Seasat Scatterometer. *J. Phys. Oceanogr.*, **20**, 1175–1205.

Cox, M. D., 1984: A primitive equation, 3-dimensional model of the ocean. Techn Rep. 1, Ocean Group, Geophys. Fluid Dyn. Lab., Princeton, NJ.

——, 1985: An eddy resolving numerical model of the ventilated thermocline. *J. Phys. Oceanogr.*, **15**, 1312–1324.

Gill, A. E., and P. P. Niiler, 1973: The theory of seasonal variability in the ocean. *Deep-Sea Res.*, **20**, 141–177.

Gordon, A., 1986: Interocean exchange of thermocline water. *J. Geophys. Res.*, **91**, 5037–5046.

Greatbatch, R. J., and A. Goulding, 1989: Seasonal variations in a linear barotropic model of the North Atlantic driven by the Hellerman and Rosenstein wind stress field. *J. Phys. Oceanogr.*, **19**, 572–595.

Hall, M. M., and M. L. Bryden, 1982: Direct estimates and mechanisms of ocean heat transport. *Deep-Sea Res.*, **29**, 339–360.

Han, Y., 1984: A numerical World Ocean general circulation model, Part II. *Dyn. Atmos. Oceans,* **8,** 141–172.

Harrison, D. E., 1989: On climatological monthly mean wind stress and wind stress curl fields over the world ocean. *J. Climate,* **2,** 57–70.

Hellerman, S., and M. Rosenstein, 1983: Normal monthly wind stress over the World Ocean with error estimates. *J. Phys. Oceanogr.,* **13,** 1093–1104.

Isemer, H.-J., and L. Hasse, 1987: *The BUNKER Climate Atlas of the North Atlantic Ocean. Vol. 2: Air–Sea Interactions.* Springer-Verlag, 256 pp.

Kaufeld, L., 1981: The development of a new Beaufort equivalent scale. *Meteor. Rundsch.,* **34,** 17–23.

Large, W. G., and S. Pond, 1981: Open ocean flux measurements in moderate to strong winds. *J. Phys. Oceanogr.,* **11,** 324–336.

Larsen, J. C., and T. B. Sanford, 1985: Florida Current volume transports from voltage measurements. *Science,* **227,** 302–304.

Leaman, K. D., R. L. Molinari and P. S. Vertes, 1987: Structure and variability of the Florida Current at 27°N: April 1982–July 1984. *J. Phys. Oceanogr.,* **17,** 565–583.

——, and J. E. Harris, 1990: On the average absolute transport of the deep western boundary currents east of Abaco Islands, the Bahamas. *J. Phys. Oceanogr.,* **20,** 467–475.

Lee, T. N., and E. Williams, 1988: Wind forced transport fluctuations of the Florida Current. *J. Phys. Oceanogr.,* **18,** 937–946.

——, W. Johns, F. Schott and R. Zantopp, 1990: Western boundary current sructure and variability east of Abaco, Bahamas, at 26.5°N. *J. Phys. Oceanogr.,* **20,** 446–466.

Leetma, A., P. P. Niiler and H. Stommel, 1977: Does the Sverdrup relation account for the mid-Atlantic circulation? *J. Mar. Res.,* **35,** 1–10.

Levitus, S., 1982: Climatological Atlas of the World Ocean. NOAA Tech. Paper, **3,** 173 pp.

Molinari, R. L., E. Johns and J. F. Festa, 1990: The annual cycle of meridional heat flux in the Atlantic Ocean at 26.5°N. *J. Phys. Oceanogr.,* **20,** 476–482.

Niiler, P. P., and W. S. Richardson, 1973: Seasonal variability of the Florida Current. *J. Mar. Res.,* **31,** 144–167.

Olsen, D., F. Schott, R. Zantopp and K. Leaman, 1984: The mean circulation east of the Bahamas as determined from a recent measurement program and historical XBT data. *J. Phys. Oceanogr.,* **14,** 1470–1487.

Roemmich, D., and C. Wunsch, 1985: Two transatlantic sections: meridional circulation and heat flux in the subtropical North Atlantic Ocean. *Deep-Sea Res.,* **32,** 619–664.

Rosenfeld, L. K., R. L. Molinari and K. D. Leaman, 1989: Observed and modeled annual cycle of transport in the Straits of Florida and east of Abaco Island, the Bahamas (26.5°N). *J. Geophys. Res.,* **94**(C4), 4867–4878.

Sarmiento, J. L., 1986: On the North and Tropical Atlantic heat balance. *J. Geophys. Res.,* **91**(C 10), 11 677–11 689.

Schmitz, W. J., and W. S. Richardson, 1968: On the transport of the Florida Current. *Deep-Sea Res.,* **15,** 679–693.

——, and P. L. Richardson, 1990: On the sources of the Florida Current. *Deep-Sea Res.* (in press)

Schott, F. A., and R. Zantopp, 1985: Florida Current: Seasonal and interannual variability. *Science,* **227,** 308–311.

——, and C. W. Böning, 1990: The WOCE model in the western equatorial Atlantic: Upper-layer circulation. *J. Geophys. Res.* **96**(C4), 6993–7004.

——, T. N. Lee and R. Zantopp, 1988: Variability of structure and transport of the Florida Current in the period range from days to seasonal. *J. Phys. Oceanogr.,* **18,** 1209–1230.

Smith, S. D., 1980: Wind stress and heat flux over the ocean in gale force winds. *J. Phys. Oceanogr.,* **10,** 709–726.

Smith, L. T., D. B. Boudra and R. Bleck, 1990: A wind-driven isopycnic coordinate model of the North and Equatorial Atlantic Ocean. II: The Atlantic basin experiments. *J. Geophys. Res.,* **95**(C8), 13 105–13 128.

WMO, 1970: Reports on marine scientific affairs. Rep. No. 3. The Beaufort scale of wind force. WMO, Geneva, 22 pp.

Wunsch, C., 1984: An eclectic Atlantic Ocean circulation model, I, The meridional flux of heat. *J. Phys. Oceanogr.,* **14,** 1712–1733.

——, and D. Roemmich, 1985: Is the North Atlantic in Sverdrup balance? *J. Phys. Oceanogr.,* **15,** 1876–1880.